Tunable nanowire nonlinear optical probe

Yuri Nakayama[1,6]*, Peter J. Pauzauskie[1,5]*, Aleksandra Radenovic[2,4]*, Robert M. Onorato[1]*, Richard J. Saykally[1], Jan Liphardt[2,3,4], and Peidong Yang[1,5]

[1]Department of Chemistry, [2]Department of Physics, and [3]Biophysics Graduate Group, University of California, Berkeley, CA 94720, USA

[4]Physical Biosciences Division and [5]Materials Science Division, Lawrence Berkeley National Laboratory, Berkeley, CA 94720, USA

[6]Materials Laboratories, Sony Corporation, 4-16-1 Okata, Atsugi-shi, Kanagawa 243-0021, Japan

*These authors contributed equally to this work.

One crucial challenge for subwavelength optics has been the development of a tunable source of coherent laser radiation for use in the physical, information, and biological sciences that is stable at room temperature and physiological conditions. Current advanced near-field imaging techniques using fiber-optic scattering probes[1, 2] have already achieved spatial resolution down to the 20-nm range. Recently reported far-field approaches for optical microscopy, including stimulated emission depletion (STED)[3], structured illumination[4], and photoactivated localization microscopy (PALM)[5], have also enabled impressive, theoretically-unlimited spatial resolution of fluorescent biomolecular complexes. Previous work with laser tweezers[6-8] has suggested the promise of using optical traps to create novel spatial probes and sensors. Inorganic nanowires have diameters substantially below the wavelength of visible light and have unique electronic and optical properties[9,10] that make them prime candidates for subwavelength laser and imaging technology. Here we report the development of an electrode-free, continuously-tunable coherent visible light source compatible with physiological environments, from individual potassium niobate ($KNbO_3$) nanowires. These wires exhibit efficient second harmonic generation (SHG), and act as frequency converters, allowing the local synthesis of a wide range of colors via sum and difference frequency generation (SFG, DFG). We use this tunable nanometric light source to implement a novel form of subwavelength microscopy, in which an infrared (IR) laser is used to optically trap and scan a nanowire over a sample, suggesting a wide range of potential applications in physics, chemistry, materials science, and biology.

Nanometer-scale photonics is emerging as a key ingredient for novel sensing and imaging applications, as well as for advanced information technology, cryptography, and signal processing circuits. A key requirement for a versatile and useful nonlinear circuit element for integrated optical networks is the ability to frequency-double light via SHG, a second-order nonlinear optical phenomenon. In this process, two photons with the fundamental angular frequency ω_1 are converted through a nonlinear crystal polarization into a single photon ω_2 at twice the fundamental frequency ($\omega_2 = 2\omega_1$). We have recently demonstrated and characterized harmonic generation[11], waveguiding, and optically

pumped lasing in single nanowires of zinc oxide (ZnO)[12] and gallium nitride[13]. Despite the growing availability of building blocks such as light-emitting diodes[10,14] lasers[13,15,16], photodetectors[17], and waveguides[18], the field still lacks sufficiently small devices that efficiently generate tunable coherent photons. In this study, we demonstrate that the large second-order susceptibility, $\chi^{(2)}$, of $KNbO_3$ nanowires facilitates the generation of tunable, coherent visible radiation that is sufficient for *in situ* scanning and fluorescence microscopy.

We chose the perovskite-oxide $KNbO_3$ as the nanowire material due to its low toxicity, chemical stability, large effective nonlinear optical coefficients (d_{eff}=10.8 ~ 27pm/V at λ=1064 nm) at room temperature[19], large refractive indices (n=2.1~2.5)[20], as well as its transparency in a wide range of wavelengths including the visible spectral region[21]. Single crystalline $KNbO_3$ nanowires were synthesized using a hydrothermal method[22], and characterized as orthorhombic phase (Amm2) with the growth axis parallel to the [011] direction (**Fig. 1a-e**): the polar *c*-axis[23] is therefore 45 degrees off the nanowire's growth axis.

The SHG response of single $KNbO_3$ nanowires were characterized first using femtosecond pulses described elsewhere[24] and compared with measurements of ZnO nanowires which have been studied previously[11]. The nanowires were supported on amorphous silica coverslips and aligned such that the growth axis was orthogonal to the pump beam. The maximum SHG signals for both $KNbO_3$ and ZnO nanowires (λ=502nm) are shown in **Fig. 1f**, generated by introducing the fundamental beam (λ=1004 nm, 18kW/cm^2). A direct comparison of the SHG signal collected from single $KNbO_3$ and ZnO nanowires is complicated by the anisotropic scattering related to their respective rectangular and hexagonal cross sections. However, a rough estimate for the d_{eff} of $KNbO_3$ nanowires based on the relative ratio of integrated signals is possible and found to be ~9.1pm/V. This illustrates that the nonlinear polarizability of $KNbO_3$ nanowires is larger than that for ZnO, as expected from consideration of bulk values.

The second key requirement for a versatile nonlinear circuit element for use in nano-photonics is wave mixing, specifically SFG ($\omega_3 = \omega_1 + \omega_2$) and DFG ($\omega_3 = |\omega_1 - \omega_2|$). **Fig. 1g** shows SFG signals (λ = 423nm, 454nm) and as well as SHG signals (λ = 525nm, 700nm) obtained from a single $KNbO_3$ nanowire by introducing fundamental beams at a variety of different frequencies via the tunable femtosecond pump. This demonstrates the ability of nanowire frequency converters to create four different waves from two fundamental input frequencies ω_1 and ω_2: $2\omega_1$, $2\omega_2$, and $|\omega_1 \pm \omega_2|$. The DFG signal corresponding to the SFG at 423nm was not observed here because the expected wavelength (λ=7200nm) is outside of current instrumental limits. The SHG signal at 400 nm was weak due to photoabsorption within the nanowire. This set of experiments demonstrates the ability of $KNbO_3$ nanowires to generate continuously-tunable and coherent light throughout the visible spectrum via nonlinear wave mixing. This capability, as well as the nanowire's subwavelength cross-section, enables the development of a novel form of scanning light microscopy.

Recently, laser trapping was used to optically manipulate nanowires in closed aqueous chambers[8,25]. We hypothesized that a single $KNbO_3$ nanowire may, when optically trapped, be able to frequency-double the trapping light and then waveguide this locally generated light to its ends. Single $KNbO_3$ nanowires were optically trapped using a home-built infrared[8] optical tweezers instrument (**Fig. 2a**) with the trap wavelength at 1064 nm, a popular wavelength for optical trapping of wet samples due to the tolerance of living cells to IR laser irradiation[26]. An electron-multiplying CCD was used to search for visible light radiating from trapped nanowires.

As hoped, light was observed to radiate from the distal end of trapped $KNbO_3$ nanowires. We charted the radiation profile as a function of position along the nanowire's long axis by coarsely changing the focus of the top objective mounted on a micrometer stage (**Fig. 2b**). A diffraction-limited spot was observed at the distal end of the wire, revealing optical waveguiding away from the site of photon conversion and emission from the aperture defined by the nanowire's cross-section. Measurements with a color CCD

camera show that SHG output from the nanowire varies less than 0.2% from the mean over >20 seconds of collection (Supporting Information, **Fig. S3a**).

The light emitted from the nanowire's end was collected through the lower trapping objective and spectrally analyzed. Spectral analysis revealed that the light was green with a wavelength of 531 ± 1.8 nm (**Fig. 2b**), matching well with the expected SHG signal given a trapping/pump wavelength of 1064nm. As a control, we also trapped ZnO and Si nanowires. ZnO (not shown) and Si nanowires (**Fig. 2c**, black line) did not produce visible light, supporting our assignment of the green light from the $KNbO_3$ nanowires as light generated inside the nanowire by SHG and indicating negligible SHG from symmetry breaking at the wire-water interface.

Assuming a non-depleted plane-wave pump geometry (Supporting Information) and a typical trap irradiance of ~10^8 W/cm^2, the total 2-photon conversion efficiency, $\eta_{2\omega}$, is calculated to be at least 10^{-5}. Estimations from this simple theoretical model are in agreement with second harmonic output powers of ~10 nW measured with the electron multiplying CCD (Supporting Information). Although we used a 1064nm laser, there is no theoretical limitation to extending both trapping and second harmonic generation to the range of wavelengths demonstrated above with femtosecond pulses.

Unlike other nonlinear optical geometries where alignment is accomplished manually via transducers, here the nonlinear crystal (the nanowire) spontaneously orients itself to the optical axis of the trap/pump laser resulting in detectable SHG signal along the [011] growth axis. This favorable index matching allows the entire nanowire cavity to participate in the production of second harmonic photons. It is possible that index matching could be further improved by controlling the temperature of the buffer, although we did not explore this here.

Having in hand a nanometric, raster-scannable source of coherent visible light, we wondered whether it could be used to image objects. We used a simple transmission geometry analogous to NSOM[27, 28] (near-field scanning optical microscopy), in which the

sample is scanned through a beam, modulating the fraction of light arriving at a detector. The ultimate resolution of such a transmission microscope depends on the radiation characteristics of the illumination source. In this approach the resolution is on order of the cross-section of the illumination aperture but many other factors are also important, such as the quality the probe's end-facets, far-field collection optics, and implemented feedback control.

To see if radiating nanowires can be used to image objects and to characterize the resolution of such a 'nanowire scanning microscopy' (**Fig. 3a**), we fabricated a test pattern via electron beam lithography consisting of series of 200 nm wide, 50 nm thick lines of gold on transparent glass coverslips with decreasing pitch between each line. A 'benchmark' image of the gold pattern was obtained by AFM (**Fig. 3b**) and shows the progressively finer separation between each line, decreasing from ~1000 nm to ~200 nm (**Fig. 3c**).

The laser trap was then used to raise a single $KNbO_3$ nanowire to the top coverslip surface with the gold pattern while a piezoelectric stage with nanometer positioning resolution was used to scan the pattern with respect to the wire. Each time the trapped wire passed over a gold feature there was a reduction of transmitted second harmonic emission. Scanning the nanowire tip directly across the surface resulted in a transmitted intensity map with local spatial resolution on the order of the wire's diameter (**Fig. 3d**). Measurements of the pitch between lines within the gold pattern were made for both AFM and nanowire optical transmission line scans and remarkably agreed to within ~10% (Supporting Information, **Table S1**). As expected, the minimum resolvable feature-size (pitch) decreases as the cross-section of the nanowire-probe decreases (Supporting Information, **Fig. S2c,f**).

The overall resolution in these experiments is reduced by the use of far-field optics for image collection and (presumably) the fluctuations of the nanowire in the optical potential. Root-mean-square lateral displacements of the wire due to thermal fluctuations in the optical potential are estimated to be ~10 nm by measurement of the power

spectrum of a trapped wire using a position sensitive photodetector[8] (Supporting Information, **Fig. S1d**); longitudinal fluctuations will be larger due to reduced confinement of the wire along the optical axis. Indeed, one of the most pressing next steps in the development of nanowire scanning microscopy will be to find ways of reducing longitudinal fluctuations; a theoretically ideal probe would be tapered, since this would increase optical confinement and also the crystal volume in the region of largest field intensity.

In addition to exploring this scanning transmission mode, it is also possible to investigate this new scanning probe in a fluorescence mode. We optically trapped a single $KNbO_3$ nanowire and touched its distal end to a fluorescent bead (**Fig. 4a**). In some instances, wires adhered to the bead at the contact point presumably due to the bead's carboxylate surface functionalization (for adhesion to the top coverslip). Excitation occurred in this near field geometry which generated a distinct orange fluorescence at the contact point (**Fig. 4c**). Removal of the nanowire reduced orange emission from the bead by > 80 fold (**Fig. 4d**), indicating that the 532 nm SHG emitted by the nanowire was the predominant source of excitation relative to 2-photon fluorescence. **Fig. 4e** shows the intensity difference between **Fig. 4c** and **d** from digital subtraction of the red components of the images, which displays the distinctive fluorescence emission due to SHG-excitation from the optically trapped $KNbO_3$ nanowire.

The next step in the development of nanowire-scanning microscopy will be to adapt the by now highly-refined signals -processing and -deconvolution algorithms originally developed for AFM and NSOM to this new method. Although already providing promising lateral resolution (**Fig. 3**), the utility of nanowire scanning microscopy will further increase once it is understood how to convolve and best interpret the various readouts (fraction of excitation light transmitted, sample fluorescence emission), and the mechanical deflection of the nanowire as it is tapped over a sample, as measured from scattering between the trapping laser[29, 30] and the nanowire. Similar to NSOM, nanowire scanning microscopy is an inherently mechano-optical form of microscopy since the mechanical probe (the nanowire) also functions as a source of coherent visible radiation.

One potential advantage of nanowire scanning microscopy is its extension to massively parallel excitation arrays using holographic optical elements[25] that would be compatible with sealed environments, such as microfluidic chambers.

METHODS SUMMARY

$KNbO_3$ nanowires were synthesized using a hydrothermal method[22]. For nonlinear wave mixing measurements, SFG spectra (**Fig. 1f-g**) were collected by introducing two fundamental beams with the same polarization directions[11]. Nanowire optical trapping was performed according to Ref. 8. The continuous-wave IR laser (λ = 1064 nm, ~1 W) was introduced from the bottom side of the chamber to trap the nanowire as well as to generate the second harmonic wave at λ = 532 nm. The trapping instrument was modified with a color CCD (**Fig. 2a**) to acquire images of optically trapped $KNbO_3$ wires at various focal planes by moving the top objective along the optical axis without translation of the trapping point. Spectra were taken through the bottom objective. Gold surface-patterns were made for the scanning measurements using glass coverslips coated with a 2 nm chromium bonding layer. Electron beam lithography was used to define ~200 nm wide lines with variable pitch. Thermal evaporation of gold yielded ~50 nm thick lines of gold. Transmitted SHG signal was collected with a high-speed electron-multiplying CCD camera (Andor, iXon), and custom software written in C++ was used to control the scan size and speed of the xyz-piezo stage. Fluorescent polystyrene beads containing POPO-3 dye molecules were fixed to the surface of a glass coverslip via carboxylate surface functionalization. The distal end of trapped nanowire was brought in contact with one of the beads (**Fig. 4a-c**) and color CCD images were taken (Photometrics, CoolSNAPcf).

METHODS

Materials preparation. Potassium hydroxide and niobium pentoxide were mixed with deionized water for 2 hours at room temperature[22]. The slurry was transferred to Teflon vessels and then heated at 150^{o}C for 2-6 days using the stainless autoclaves. Sizes could be varied by adjusting the reaction time. Scanning electron microscopy (SEM) images showed that the products are collections of rectangularly-shaped nanowires with widths ranging from 40 to 400 nm and the lengths from 1 to 20 μm (Fig. 1a). The products were identified as the single phase orthorhombic $KNbO_3$ (Amm2, a = 0.3984 nm, b = 0.5676 nm, and c = 0.5697 nm) from X-ray powder diffraction (XRD) measurements (**Fig. 1b**). Transmission electron microscope (TEM) images and electron diffraction (ED) measurements (**Fig. 1c-e**) show that the nanowires grow parallel to [011] directions. Twinned structures were observed in some nanowires.

Nonlinear optical measurements. Single nanowire suspensions were obtained after sonication in iso-propanol and placed on a transparent glass coverslip with a nanomanipulator. Femtosecond pulses generated by a regeneratively amplified Ti:sapphire oscillator (wavelength: λ = 800 nm, 90 fs, 1 kHz) were used to pump an OPA where the wavelength is continuously tunable between 1150-2600 nm and can be frequency doubled by a BBO crystal outside the OPA providing access to shorter wavelengths before being introduced to the nanowire perpendicular to its growth direction (**Fig. 1f-g**). The beam spot size was about 1 μm, which is larger than the width of the wires but smaller than their lengths. SFG spectra were measured by introducing two fundamental beams with the same polarization directions. From the experimental configuration, coefficients are identified as $d_{eff} = d_{31}$ for $KNbO_3$ nanowire, and $d_{eff} = d_{33}$ for ZnO nanowire.

Optical trapping. Nanowires were dispersed into deionized water inside the sample chamber[3]. The continuous-wave IR laser (λ = 1064 nm, ~1 W) was introduced from the bottom side of the chamber to trap the nanowire as well as to generate the second harmonic wave at λ = 532 nm. The chamber can be moved coarsely with a manual stage, and finely with a three-axis piezostage. Color CCD images are taken at various focal planes by moving the top objective along the optical axis without translation of the trapping point, whereas spectra were taken through the bottom objective. From the experimental configuration and material properties, nonlinear optical coefficients are considered as $d_{eff} = 0$ for both ZnO and Si nanowires. SHG signal from surface inversion symmetry breaking was too small to detect in this study.

Nanowire Scanning. Gold line patterns were fabricated using electron beam lithography with glass coverslips coated with a 2 nm chromium bonding-layer. The electron beam was used to define ~200 nm wide line patterns with variable pitch. After 50 nm of thermal gold deposition, reactive ion etching (RIE) was used to remove residual chromium from glass to prevent laser heating and bubble formation during scanning measurements. Transmitted SHG signal was collected (at a frame rate of 20 Hz) by using an Andor (South Windsor, CT) iXon camera. Custom software written in C++ was used to control the scan size and speed of xyz-piezo stage (Nano-UHV100; Mad City Lab, Madison,Wisconsin, USA). During raster scanning experiments the microfabricated gold lines modulated the SHG signal transmitted through the coverslip due to a change of the local optical transparency. Future work to improve feedback during raster scanning might employ high-speed analysis of the variability in SHG output due to changes in phase matching from opto-mechanical deflections of the nanowire. All scanning data

sets were processed using custom software written Igor Pro 5 (Wavemetrics, Inc). After scanning, wires were fixed to the glass surface using non-specific binding. AFM (Asylum Research MFP3D combined with Nikon inverted microscope) operating in tapping mode was used to image fixed nanowires used in the scanning measurements as well as e-beam substrates following RIE. All AFM images were obtained with the MikroMasch probes (model no. NSC36/NoAl) nominal spring constant 0.6 N/m.

Bead excitation. Polystyrene beads (1 μm in diameter) containing the fluorescent dye POPO-3 (main emission peak ~570 nm, absorption peak ~532 nm, Molecular Probes, Fig. 3f) were fixed to the surface of a glass coverslip via carboxylate surface functionalization. The distal end of trapped nanowire is brought in contact with one of the beads (**Fig. 4a-c**) and color CCD images were taken (Photometrics, CoolSNAPcf). The initial position was set using a computer controlled piezoelectric stage. The stage could be actuated to remove the nanowire. Finally the empty laser trap was moved to the original position, for corresponding 2-photon excitation (**Fig. 4d**). The subtraction of **Fig. 4d** from **Fig. 4c** is performed using the red component of the color images. Spectra in **Fig. S4** were obtained (Acton, SpectraPro 300i) using a sample chamber filled with a 20 vol% aqueous POPO-3 dye solution. The luminescence spectrum of SHG-excitation was obtained by subtraction of pure two-photon luminescence (without trapping a nanowire) from spectra with a trapped $KNbO_3$ nanowire.

References

1. Sanchez, E. J., Novotny, L. & Xie, X. S. Near-field fluorescence microscopy based on two-photon excitation with metal tips. Physical Review Letters 82, 4014-4017 (1999).
2. Inouye, Y. & Kawata, S. Near-Field Scanning Optical Microscope With A Metallic Probe Tip. Optics Letters 19, 159-161 (1994).
3. Donnert, G. et al. Macromolecular-scale resolution in biological fluorescence microscopy. Proceedings Of The National Academy Of Sciences Of The United States Of America 103, 11440-11445 (2006).
4. Gustafsson, M. G. L. Nonlinear structured-illumination microscopy: Wide-field fluorescence imaging with theoretically unlimited resolution. Proceedings Of The National Academy Of Sciences Of The United States Of America 102, 13081-13086 (2005).
5. Betzig, E. et al. Imaging intracellular fluorescent proteins at nanometer resolution. Science 313, 1642-1645 (2006).
6. Ghislain, L. P. & Webb, W. W. Scanning-Force Microscope Based On An Optical Trap. Optics Letters 18, 1678-1680 (1993).
7. Florin, E. L., Horber, J. K. H. & Stelzer, E. H. K. 3-D scanning probe microscope based on optical tweezers and 2-photon excitation by a cw-Nd:YAG laser. Biophysical Journal 70, WP307-WP307 (1996).
8. Pauzauskie, P. J. et al. Optical trapping and integration of semiconductor nanowire assemblies in water. Nature Materials 5, 97-101 (2006).
9. Yang, P. The Chemistry and Physics of Semiconductor Nanowires. MRS Bulletin 30, 85-91 (2005).
10. Sirbuly, D. J., Law, M., Yan, H. Q. & Yang, P. D. Semiconductor nanowires for subwavelength photonics integration. Journal of Physical Chemistry B 109, 15190-15213 (2005).
11. Johnson, J. C. et al. Near-field imaging of nonlinear optical mixing in single zinc oxide nanowires. Nano Letters 2, 279-283 (2002).
12. Johnson, J. C., Yan, H. Q., Yang, P. D. & Saykally, R. J. Optical cavity effects in ZnO nanowire lasers and waveguides. Journal of Physical Chemistry B 107, 8816-8828 (2003).
13. Pauzauskie, P. J., Sirbuly, D. J. & Yang, P. D. Semiconductor nanowire ring resonator laser. Physical Review Letters 96, 14903-1-143903-4 (2006).
14. Qian, F. et al. Gallium nitride-based nanowire radial heterostructures for nanophotonics. Nano Letters 4, 1975-1979 (2004).
15. Huang, Y., Duan, X., Wei, Q. & Lieber, C. M. Directed Assembly of One-Dimensional Nanostructures into Functional Networks. Science 291, 630-633 (2001).
16. Duan, X. F., Huang, Y., Agarwal, R. & Lieber, C. M. Single-nanowire electrically driven lasers. Nature 421, 241-245 (2003).
17. Kind, H., Yan, H. Q., Messer, B., Law, M. & Yang, P. D. Nanowire ultraviolet photodetectors and optical switches. Advanced Materials 14, 158-160 (2002).
18. Law, M. et al. Nanoribbon waveguides for subwavelength photonics integration. Science 305, 1269-1273 (2004).

19. Shoji, I., Kondo, T., Kitamoto, A., Shirane, M. & Ito, R. Absolute scale of second-order nonlinear-optical coefficients. Journal of the Optical Society of America B-Optical Physics 14, 2268-2294 (1997).
20. Zysset, B., Biaggio, I. & Gunter, P. Refractive-Indexes of Orthorhombic Knbo3.1. Dispersion and Temperature-Dependence. Journal of the Optical Society of America B-Optical Physics 9, 380-386 (1992).
21. Kudo, K., Kakiuchi, K., Mizutani, K. & Fukami, T. Characterization of KNbO3 crystal by traveling solvent floating zone (TSFZ) method. Japanese Journal of Applied Physics Part 1-Regular Papers Short Notes & Review Papers 42, 6099-6101 (2003).
22. Magrez, A. et al. Growth of single-crystalline KNbO3 nanostructures. Journal of Physical Chemistry B 110, 58-61 (2006).
23. Biaggio, I., Kerkoc, P., Wu, L. S., Gunter, P. & Zysset, B. Refractive-Indexes of Orthorhombic Knbo3.2. Phase-Matching Configurations for Nonlinear-Optical Interactions. Journal of the Optical Society of America B-Optical Physics 9, 507-517 (1992).
24. Knutsen, K. P., Messer, B. M., Onorato, R. M. & Saykally, R. J. Chirped coherent anti-Stokes Raman scattering for high spectral resolution spectroscopy and chemically selective imaging. Journal of Physical Chemistry B 110, 5854-5864 (2006).
25. Agarwal, R. et al. Manipulation and assembly of nanowires with holographic optical traps. Optics Express 13, 8906-8912 (2005).
26. Ashkin, A., Dziedzic, J. M. & Yamane, T. Optical Trapping and Manipulation of Single Cells Using Infrared-Laser Beams. Nature 330, 769-771 (1987).
27. Pohl, D. W., Denk, W. & Lanz, M. Optical Stethoscopy - Image Recording with Resolution Lambda/20. Applied Physics Letters 44, 651-653 (1984).
28. Betzig, E., Trautman, J. K., Harris, T. D., Weiner, J. S. & Kostelak, R. L. Breaking the Diffraction Barrier - Optical Microscopy on a Nanometric Scale. Science 251, 1468-1470 (1991).
29. Florin, E.-L., Pralle, A., Stelzer, E. H. K. & Hörber, J. K. H. Photonic force microscope calibration by thermal noise analysis. Applied Physics A 66, 75-78 (1998).
30. Grier, D. G. A revolution in optical manipulation. Nature 424, 810-816 (2003).

Author Contributions: YN performed the synthesis and structural characterization of the $KNbO_3$ wires. YN and RO designed / performed / analyzed the wave mixing experiment. PJP & AR designed / performed / analyzed the laser trapping and nanoprobe imaging experiments.

Acknowledgements This work was supported in part by the Dreyfus Foundation and the U.S. Department of Energy (P.Y.), the University of California, Berkeley (J.L.), the Experimental Physical Chemistry Program of the National Science Foundation, and NASA (R.J.S.). Y.N. thanks SONY for a research fellowship and P.J.P. thanks NSF for a graduate research fellowship. Work at the Lawrence Berkeley National Laboratory was supported by the Office of Science, Basic Energy Sciences, Division of Materials Science of the U.S. Department of Energy. We thank T. Kuykendall for TEM observations and the National Center for Electron Microscopy for the use of their facilities, Prof. Lydia Sohn for AFM facilities, Neil Switz for comments on the manuscript, and Dr. Wenjie Liang for microfabrication of gold patterns.

The authors declare no competing financial interests. Correspondence and requests for materials should be addressed to J.L. (Liphardt@physics.berkeley.edu) or P.Y. (p_yang@berkeley.edu)

Figures.

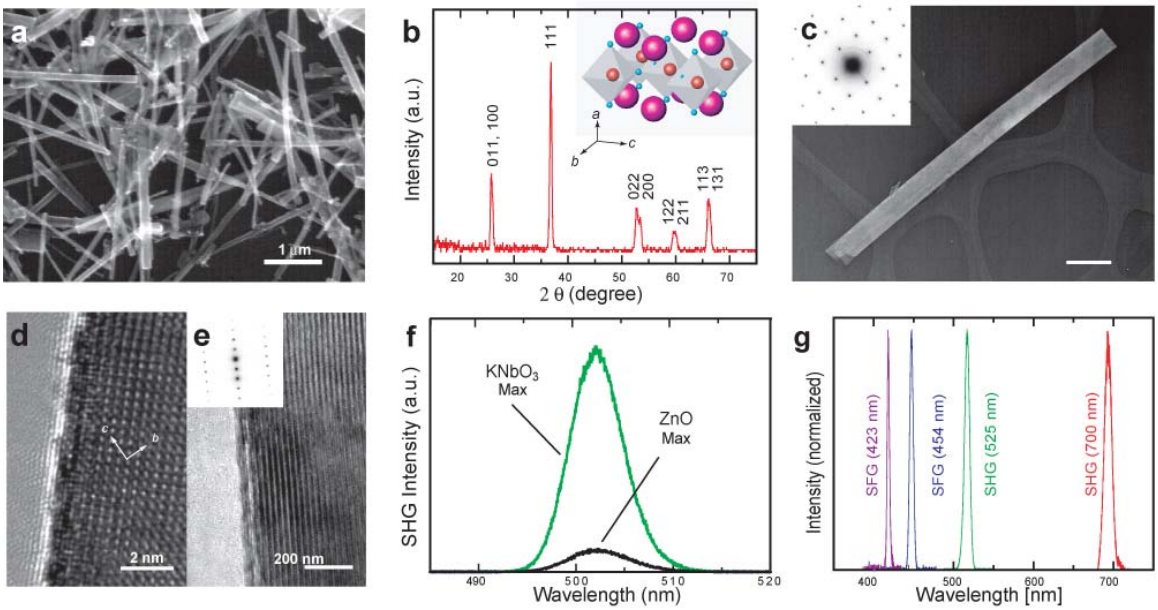

Figure 1 | $KNbO_3$ nanowires and their structural analysis. a, SEM image of $KNbO_3$ nanowires. **b,** XRD pattern of $KNbO_3$ nanowires. All peaks are indexed to orthorhombic $KNbO_3$ phase (Amm2) as indicated in the figure. Inset shows the unit cell structure of this material whose spontaneous polarization is parallel to the *c*-axis. **c,** TEM image of a $KNbO_3$ nanowire and its ED pattern (inset). The zone axis and the wire-growth direction are determined as [100] and [011] respectively. **d,e,** HRTEM images of single $KNbO_3$ nanowires and a ED pattern (**e,** inset) with the zone axis of [100] (**d**) and [2-33] (**e**). Growth directions are determined to be [011] in both images. **f,** Maximum SHG spectra of single $KNbO_3$ and ZnO nanowires (λ_{pump} = 1004 nm, 18 kW/cm^2) reflecting the larger nonlinear polarizibality of $KNbO_3$. **g,** Panchromatic wavelengths generated by the nonlinear optical processes within individual $KNbO_3$ nanowires. λ = 423 nm was produced as a result of SFG: $(423\text{ nm})^{-1} = (800\text{ nm})^{-1} + (900\text{ nm})^{-1}$, and other spectra were obtained as SFG: $(454)^{-1} = (800)^{-1} + (1050)^{-1}$, SHG: $(525)^{-1} = 2(1050)^{-1}$, and $(700)^{-1} = 2(1400)^{-1}$.

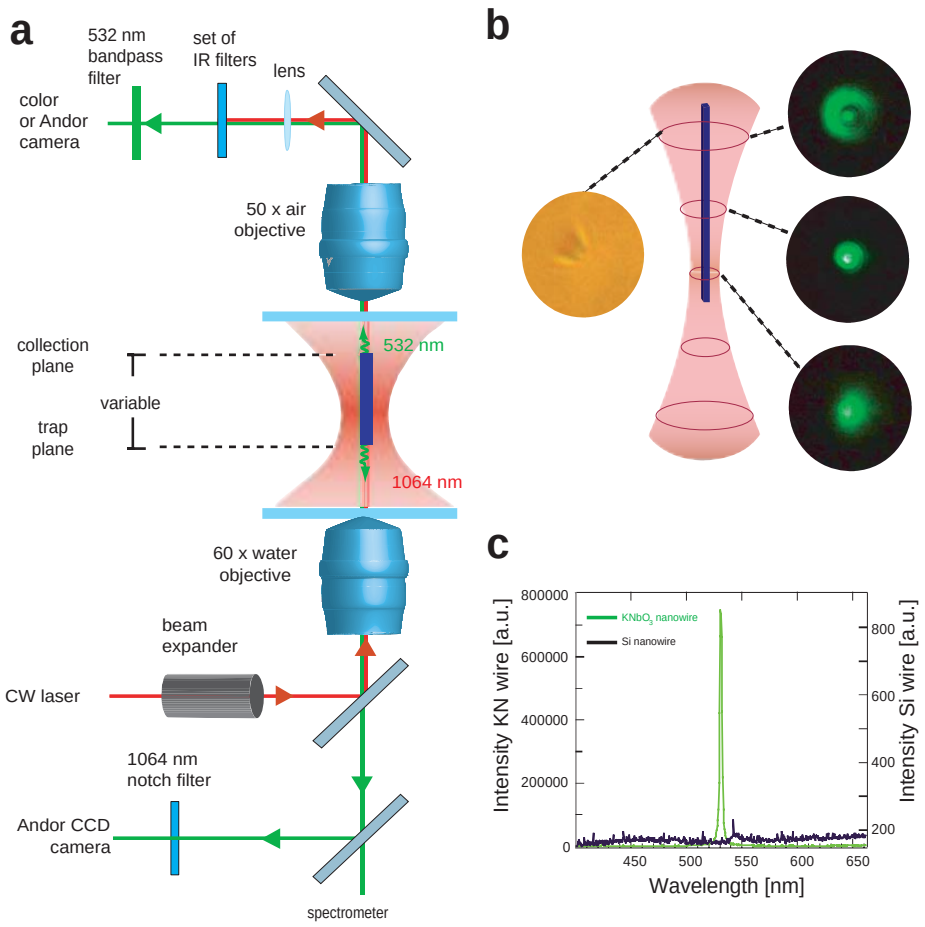

Figure 2. Radiation from optically trapped single $KNbO_3$ nanowires. a, Detailed setup for the single-beam optical trapping instrument. **b,** Bright field (left) and SHG (right) images of the trapped $KNbO_3$ nanowire. Waveguiding of the SHG signal (green) leads to diffraction rings at the distal (top) end of the nanowire which acts as a subwavelength aperture. **c,** Observed spectra for $KNbO_3$ and Si nanowires. Strong SHG signal at λ = 532 nm is collected from the trapped $KNbO_3$ nanowire (green, left axis), while no signal was observed from Si nanowires (black, right axis).

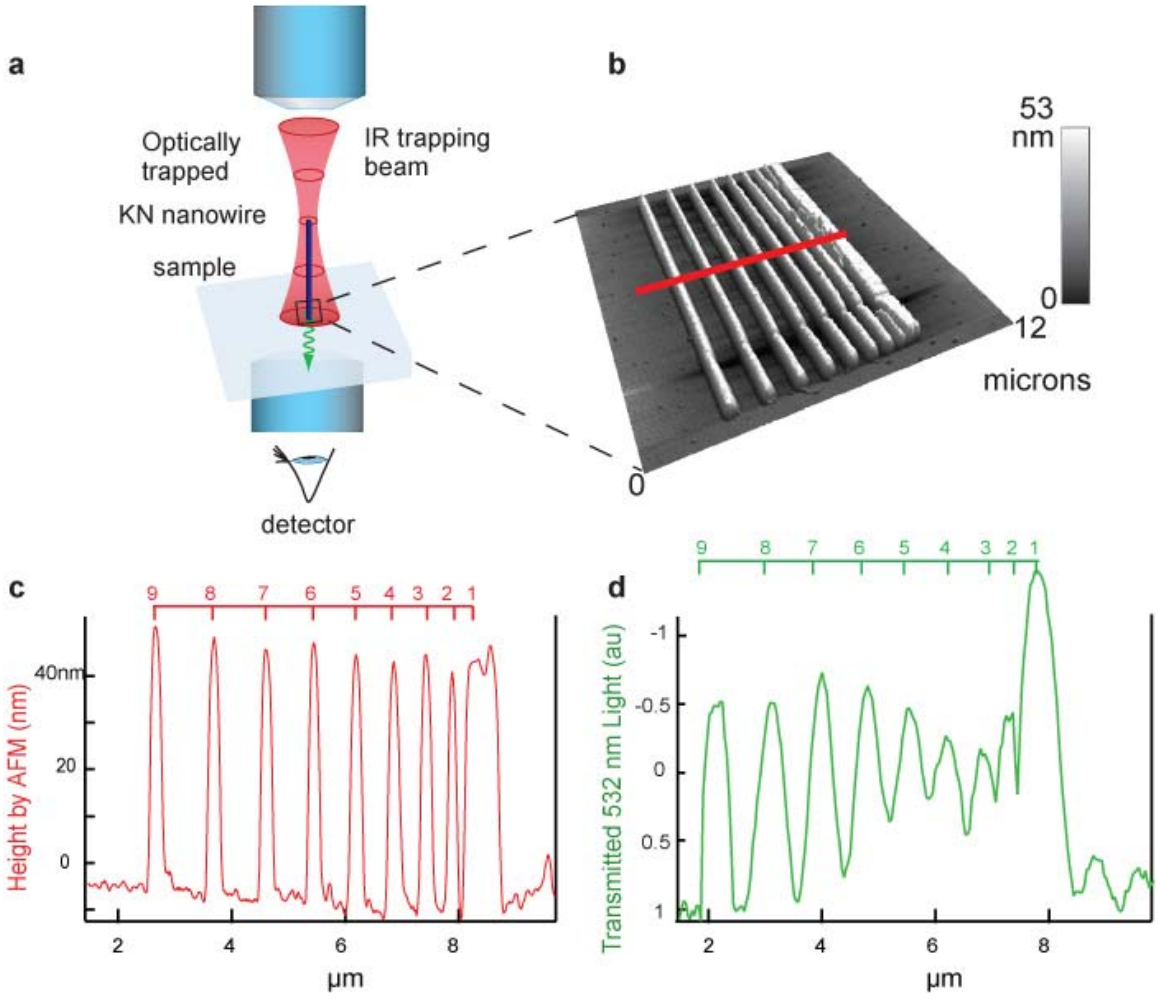

Figure 3 | Transmission line scan of metallic surface pattern with laser trapped $KNbO_3$ nanowire. a, Schematic of inverted optical scanning configuration. **b,** AFM topographic image of thermally evaporated pattern of gold stripes on a glass coverslip. **c,** AFM line scan from region indicated in (b) **d,** Optical transmission profile captured by scanning a single $KNbO_3$ nanowire over the metallic surface structure. The nanowire used to create the transmission line scan was measured by AFM to have the dimensions: width=122 nm, length =1.4 μm and height=53 nm.

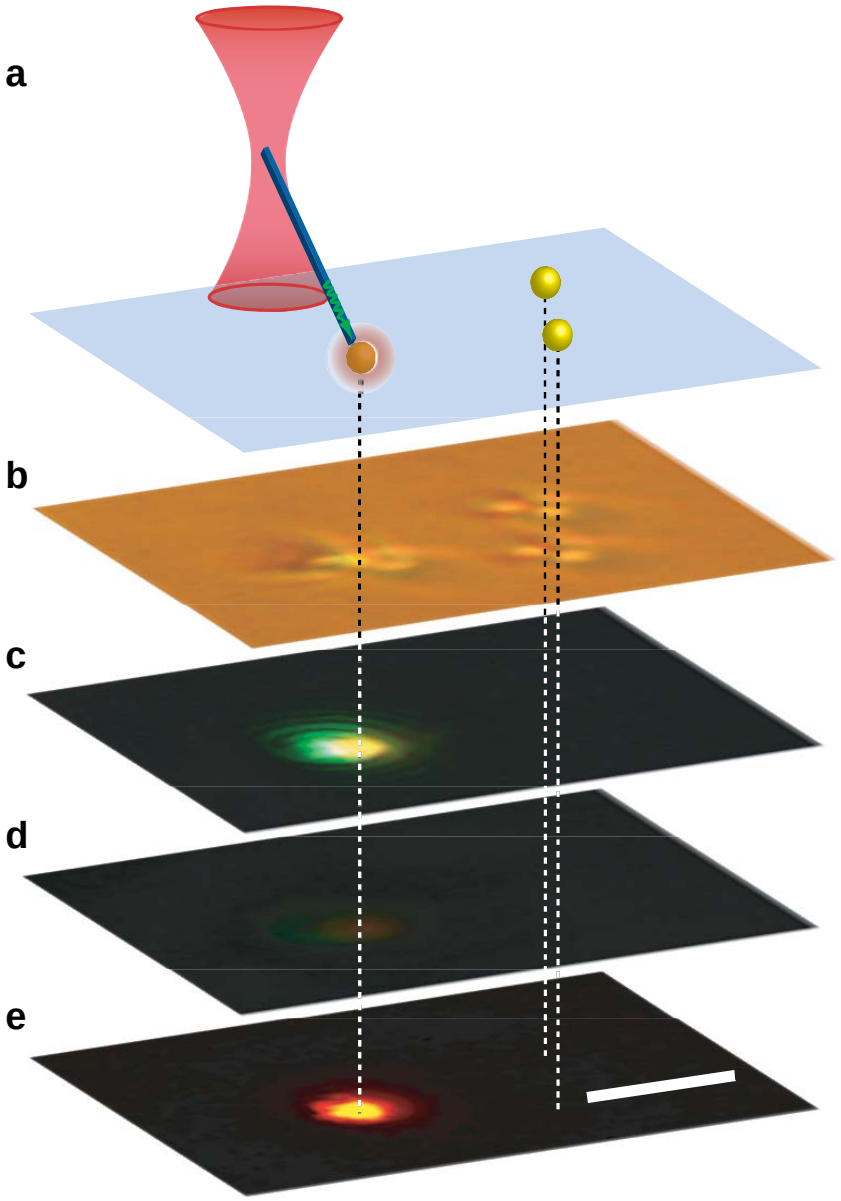

Figure 4 | POPO-3 bead excitation by waveguided SHG signal from an optically trapped $KNbO_3$ nanowire. **a,** Inverted schematic drawing of the experimental configuration. **b,** Bright field optical image of the beads, with the nanowire in contact with the leftmost bead. **c,** Color-CCD fluorescence image of (b), showing green light emission from the nanowire and the orange emission from the bead. **d,** Control image of the same beads with IR radiation in the plane from (b), but without a trapped nanowire. **e,** Digital subtraction of (d) from (c). Scale bar =3μm.

WORD COUNTS: intro: 236 body: 1829 Meth. Sum.: 252
references: 30 acknowledgment/captions: 600
methods: 818 author contribuations: 38